Physics of Fluids

Application of the Lambert W function to steady shearing Newtonian flows with logarithmic wall slip

Cite as: Phys. Fluids **32**, 053107 (2020); https://doi.org/10.1063/5.0009968
Submitted: 07 April 2020 . Accepted: 05 May 2020 . Published Online: 21 May 2020

Rafaella Pitsillou, Alexandros Syrakos, and Georgios C. Georgiou

Physics of Fluids ARTICLE scitation.org/journal/phf

Application of the Lambert W function to steady shearing Newtonian flows with logarithmic wall slip

Cite as: Phys. Fluids 32, 053107 (2020); doi: 10.1063/5.0009968
Submitted: 7 April 2020 • Accepted: 5 May 2020 •
Published Online: 21 May 2020

View Online Export Citation CrossMark

Rafaella Pitsillou,[1,a)] Alexandros Syrakos,[2,b)] and Georgios C. Georgiou[3,c)]

AFFILIATIONS

[1] Department of Physics, University of Cyprus, P.O. Box 20537, 1678 Nicosia, Cyprus
[2] Department of Mechanical and Manufacturing Engineering, University of Cyprus, P.O. Box 20537, 1678 Nicosia, Cyprus
[3] Department of Mathematics and Statistics, University of Cyprus, P.O. Box 20537, 1678 Nicosia, Cyprus

[a)] **E-mail:** pitsillou.rafaella@ucy.ac.cy
[b)] **E-mail:** alexandros.syrakos@gmail.com
[a)] **Author to whom correspondence should be addressed:** georgios@ucy.ac.cy

ABSTRACT

We consider various viscometric flows of a Newtonian fluid, i.e., plane, annular, and circular Couette flows and planar and axisymmetric Poiseuille flows, in the presence of wall slip that follows a logarithmic slip law. We derive analytical solutions in terms of the Lambert W function. The effects of logarithmic slip on these flows are discussed, and comparisons of the results with their Navier-slip counterparts are made.

I. INTRODUCTION

The no-slip condition in fluid mechanics requires that the fluid particles adjacent to a wall acquire the velocity of the wall. Hence, if the wall is fixed, the velocity of these particles is zero. The no-slip boundary condition has been widely used in modeling and solving fluid mechanics problems. However, the possibility of slip has also been noted since the early stages of development of fluid mechanics.[1] In the past few decades, experimental as well theoretical studies have demonstrated that this condition is violated in many important industrial processes not only with complex non-Newtonian fluids[1–4] but also with Newtonian liquids.[5] In his review, Hatzikiriakos[1] provides references of experimental observations of wall slip exhibited by several classes of complex fluids, such as suspensions, dispersions, gels, and foams, and discusses various mechanisms for slip. Wall slip has also been recognized as a major factor affecting the stability of certain polymer processes, such as extrusion[1,2] as well as the accuracy of rheometric experiments, e.g., with rotational rheometers. Slip is also of great importance in microfluidics and nanofluidics.[6,7]

In general, the relative velocity of the fluid with respect to that of the adjacent wall, referred to as the slip velocity, u_w^*, depends on the shear and normal wall stresses, the pressure, the temperature, the properties of the fluid, and the properties of the wall/fluid interface.[8] Navier[9] proposed the following slip law:

$$u_w^* = \frac{\tau_w^*}{\beta^*}, \tag{1}$$

where τ_w^* is the wall shear stress and β^* is the slip parameter, which encompasses the effects of all the other aforementioned material parameters. Note that throughout this paper, dimensional and dimensionless quantities are denoted by starred and starless symbols, respectively. Obviously, the no-slip boundary condition is a limiting case of Eq. (1) when $\beta^* \to \infty$. The slip or extrapolation length, l^*, defined as the distance from the wall at which a linear velocity profile is extrapolated to zero, is related to the slip parameter β^* by means of $l^* \equiv \eta^*/\beta^*$, where η^* is the (local) viscosity of the fluid. Obviously, the no-slip boundary condition corresponds to the zero extrapolation length.

A number of other more involved slip equations have been proposed in the literature. The immediate generalizations of Eq. (1) are the power-law or non-linear Navier slip law[10]

$$u_w^* = \frac{\tau_w^{*s}}{\beta^*}, \tag{2}$$

where s is the exponent ($s = 1$ in Navier slip), and the two-branch slip equation

$$u_w^* = \begin{cases} 0 & \tau_w^* \le \tau_c^* \\ \frac{(\tau_w^* - \tau_c^*)^s}{\beta^*} & \tau_w^* > \tau_c^*, \end{cases} \tag{3}$$

where τ_c^* is slip or sliding or threshold yield stress.[11,12] The exponent s depends on the properties of the lubricated films at the material/wall interface. In the case of suspensions in solvents following the power-law constitutive equation, s is equal to the corresponding power-law exponent. Hence, with a Newtonian solvent, $s = 1$, and Navier slip is recovered from Eq. (2) (see Ref. 12 and references therein). The slip yield stress is the critical wall shear stress above which slip is observed with certain complex and even Newtonian fluids (Ref. 13 and references therein). The Navier slip law is recovered by setting $s = 1$ and $\tau_c^* = 0$.

Hatzikiriakos[14] proposed a slip equation with the slip yield stress extending Eyring's theory of liquid viscosity to polymer molecules, which at constant temperature can be written as follows:

$$u_w^* = \begin{cases} 0 & \tau_w^* \le \tau_c^* \\ k_1^* \sinh\left[k_2^*(\tau_w^* - \tau_c^*)\right] & \tau_w^* > \tau_c^*, \end{cases} \tag{4}$$

where k_1^* and k_2^* are positive slip parameters.

The following logarithmic law has also been employed:[15]

$$u_w^* = k_1^* \ln\left(1 + k_2^* \tau_w^*\right). \tag{5}$$

The latter slip law is referred to as the asymptotic slip law by Ferrás *et al.*[16] who indicated that the slip parameters k_1^* and k_2^* allow the adjustment of the amount of slip and of the shape of the curve $\tau_w^* - u_w^*$ to experimental data. It should be noted that when $k_2^* \tau_w^* \ll 1$, Eq. (5) is simplified to

$$u_w^* \simeq k_1^* k_2^* \tau_w^*, \tag{6}$$

which is equivalent to the Navier slip law (1) with $\beta^* = 1/(k_1^* k_2^*)$. This is also illustrated in Fig. 1, where the slip velocity is scaled by k_1^* and the wall shear stress is scaled by k_2^{*-1}.

The analysis of rheological data is not straightforward in the presence of wall slip, since the latter should be corrected for slip effects.[1,3] As pointed out by Hatzikiriakos,[1] wall slip is necessary in explaining the mismatch of rheological data obtained using different rheometers. Therefore, investigating the effects of slip is important, even in simple rheometric flows, such as the simple shear and circular Couette flows. Analytical solutions of rheometric flows in the presence of wall slip obeying the Navier slip law in Eq. (1) or its power-law and slip-yield-stress generalizations in Eqs. (2) and (3), respectively, have been reported by various researchers.

Ferrás *et al.*[16] derived analytical solutions for Newtonian and inelastic non-Newtonian flows with wall slip using the Navier slip, the power-law, and Hatzikiriakos's slip laws, i.e., Eqs. (1), (2), and (4). More specifically, they solved the plane Couette (or plane shear), the plane Poiseuille, and the plane Couette–Poiseuille flows of Newtonian, power-law, Bingham, Herschel–Bulkley, Sisko, and Robertson–Stiff constitutive models. The flows considered are basic rheometric flows. In the case of the plane Couette flow, Ferrás *et al.*[16] considered the possibility of having different slip laws at the two walls or slip only along the fixed plate.

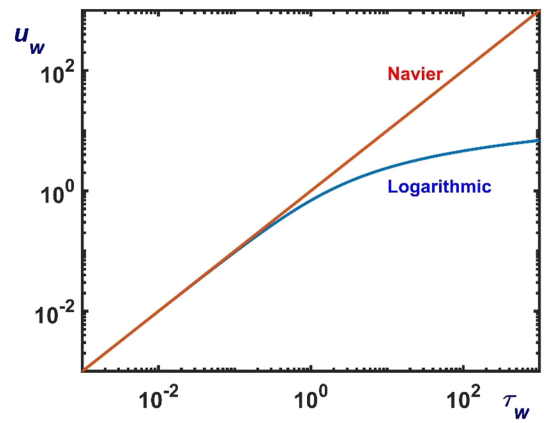

FIG. 1. Comparison of the logarithmic and Navier slip laws when $\beta^* = 1/(k_1^* k_2^*)$. The slip velocity is scaled by k_1^*, and the wall shear stress is scaled by k_2^{*-1}.

Analytical solutions with non-zero slip yield stress [i.e., using Eq. (3)] have been reported by Kaoullas and Georgiou[17] for Newtonian Poiseuille flows in planar, cylindrical, annular, and rectangular tubes. The different flow regimes defined by the critical pressure gradients required for slip to occur at a wall have also been discussed.[17] Philippou *et al.*[18] solved both the plane and circular Couette flows of a Newtonian fluid using the linear version of Eq. (3) ($s = 1$) and reported both the steady-state and the cessation solutions. Damianou *et al.*[13] employed the same slip equation to obtain solutions of the circular Couette flow of Bingham-plastic materials and determine the critical angular velocities defining the different flow regimes that arise depending on the relative values of the yield stress and the slip yield stress.

The objective of the present work is to derive analytical solutions of Newtonian rheometric flows in the presence of slip obeying the logarithmic slip Eq. (5). To our knowledge, such solutions have not been reported in spite of the plethora of solutions in the literature. As discussed below, the derivation of analytical solutions in the presence of logarithmic slip can be achieved by means of the Lambert W function.[19]

The rest of this paper is organized as follows: The definition and the basic properties of the W function are briefly presented in Sec. II, and then, the solutions of certain algebraic equations relevant to this work are derived. The literature of applications of the W function in fluid mechanics is also reviewed. In Sec. III, the plane Couette flow of a Newtonian fluid is solved employing different slip equations at the two walls or allowing the possibility of logarithmic slip only along one of the plates. The latter scenario is relevant in experiments where slip at one wall may be suppressed by using different wall materials and roughening the wall[20] or when slip is enhanced by means of wax coatings.[21] It has also been used in analytical and numerical studies.[16,22,23] In Sec. IV, the results for plane and axisymmetric Poiseuille flows are briefly summarized. The Lambert W function is not encountered when solving for the velocity and the volumetric flow rate. However, it appears if one solves for the pressure gradient in terms of the volumetric flow rate. In Sec. V, we solve the annular Couette flow, i.e., the flow in an infinitely long annulus driven by the steady axial motion of the inner cylinder. The general case of logarithmic slip along both the cylinders is not amenable to an analytical solution. Thus, we considered the cases where logarithmic slip occurs along one of the cylinders and Navier slip occurs along the other. In Sec. VI, the circular Couette flow is investigated assuming again that logarithmic slip occurs along only one of the two cylinders. Finally, some concluding remarks are provided in Sec. VII.

II. LAMBERT W FUNCTION

The Lambert function, denoted by $W(x)$, is defined as the multivalued inverse of

$$y = xe^{x} \Leftrightarrow x = W(x)e^{W(x)}. \tag{7}$$

It turns out that $W(x)$ has two branches in the real plane with a branching point at $(-1/e,\ -1)$. The principal branch, denoted by $W_0(x)$, is the upper branch in the interval $[-1/e,\ \infty)$, and the secondary branch, denoted by $W_{-1}(x)$, is the lower branch in the interval $[-1/e,\ 0)$. The principal branch maps the positive real axis onto itself, and W_0 is commonly abbreviated by W. The Lambert function has been discussed in detail by Corless *et al.*[19] who also provided application examples in various fields in applied sciences and in engineering.

The Lambert W function has been employed by different researchers in deriving analytical solutions in both Newtonian and non-Newtonian fluid mechanics. Keady[24] and later More[25] derived an analytical solution of the Colebrook and White equation for the Fanning friction factor in the turbulent flow regime. The latter author also presented a solution in terms of W for the pressure drop in the case of the steady, unidirectional ideal gas flow in a straight pipe. Jaishankar and McKinley[26] employed W to derive analytical solutions to the extended Navier–Stokes equations for the pressure and velocity profiles in gas flow through a rectangular micro-channel. Massalha and Digilov[27] described a simple, educational capillary viscometer for Newtonian fluids without the known density based on the variation of air pressure and analytically derived the time-dependent pressure in terms of the Lambert function. Pudasaini[28] reported an analytical solution for steady state debris flow fronts, where the force balance is maintained between macroviscous forces, gravity, and the hydraulic pressure gradient.

You *et al.*[29] reported approximate analytical solutions of the planar and axisymmetric Poiseuille flows of a Bingham plastic obtained using the Papanastasiou regularization model, which is inverted using the Lambert W function. They also noted that the circular Couette flow of the regularized Bingham model requires a numerical solution, in general. However, the Lambert function can still be applied to get analytical expressions for the radius of the yielded region in annular and circular Couette flows of ideal Bingham plastics.[30,31]

Below, we derive the solutions of two algebraic equations, which will be utilized to obtain analytical solutions in subsequent Secs. III–VI. First, we consider the equation

$$\ln y + Ay = B, \quad A \neq 0, \tag{8}$$

where A and B are constants, from which we get

$$e^{\ln y + Ay} = e^{B} \Rightarrow Aye^{Ay} = Ae^{B} \Rightarrow Ay = W\left(Ae^{B}\right) \Rightarrow y = \frac{1}{A}W\left(Ae^{B}\right). \tag{9}$$

Consider now the four-parameter equation

$$Ay + B = \ln(Cy + D), \quad A, C \neq 0. \tag{10}$$

This can be rearranged in the form of Eq. (8),

$$\frac{A(Cy+D)}{C} - \frac{AD}{C} + B = \ln(Cy+D) \Rightarrow \ln(Cy+D) - \frac{A}{C}(Cy+D) = B - \frac{AD}{C}.$$

Using Eq. (9) and solving for y one gets

$$y = -\frac{1}{A}W\left(-\frac{A}{C}e^{B-\frac{AD}{C}}\right) - \frac{D}{C}. \tag{11}$$

III. PLANE COUETTE FLOW

We consider the steady flow of a Newtonian fluid contained between infinite, horizontal parallel plates, assuming that the upper plate moves horizontally at a speed V^* and the lower one is fixed, as illustrated in Fig. 2. Working in Cartesian coordinates (see Fig. 2) and integrating the x-momentum equation for this unidirectional flow, one finds that the velocity and the shear stress are given by Papanastasiou *et al.*,[32]

$$u_x^*(y^*) = c_1^* y^* + c_2^* \text{ and } \tau_{yx}^* = \eta^* c_1^*, \tag{12}$$

where c_1^* and c_2^* are integration constants determined from the boundary conditions. In the general case where slip occurs at both plates, the boundary conditions read

$$u_x^*(0) = u_{w1}^* \text{ and } u_x^*(H^*) = V^* - u_{w2}^*, \tag{13}$$

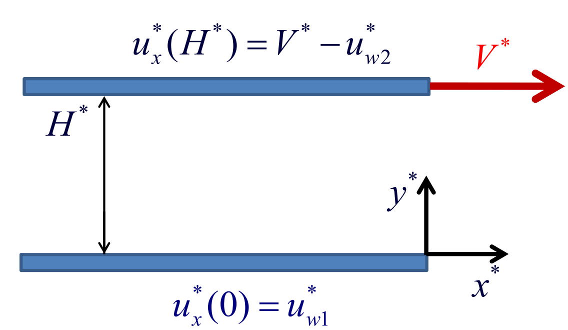

FIG. 2. Geometry and boundary conditions of the plane Couette flow with slip along both walls.

where u^*_{w1} and u^*_{w2} are the slip velocities at the lower and upper plate, respectively, and H^* is the gap width. Calculating the integration constants, one finds that

$$u^*_x(y^*) = (V^* - u^*_{w1} - u^*_{w2})\frac{y^*}{H^*} + u^*_{w1} \tag{14}$$

and

$$\tau^*_{w1} = \tau^*_{w2} = |\tau^*_{yx}| = (V^* - u^*_{w1} - u^*_{w2})\frac{\eta^*}{H^*}. \tag{15}$$

Equations (14) and (15) are general in the sense that the slip equations at the two walls have not been specified yet. The special cases for no-slip at either wall are recovered by simply zeroing the corresponding slip velocity. We now allow the possibility of different logarithmic slip equations at the two walls so that

$$u^*_{w1} = k^*_1 \ln(1 + k^*_2 \tau^*_{w1}) \tag{16}$$

and

$$u^*_{w2} = k'^*_1 \ln(1 + k^*_2 \tau^*_{w2}), \tag{17}$$

where k^*_1 and k'^*_1 are the first slip coefficients at the lower and upper walls, respectively. Note that we have chosen the second slip coefficient k^*_2 to be the same at both walls for otherwise the flow problem is not amenable to the analytical solution. Given that the shear stress is constant and thus $\tau^*_{w1} = \tau^*_{w2}$, combining Eqs. (15)–(17) gives

$$\ln(1 + k^*_2 \tau^*_{w1}) = -\frac{H^*}{\eta^*(k^*_1 + k'^*_1)}\tau^*_{w1} + \frac{V^*}{k^*_1 + k'^*_1}. \tag{18}$$

Equation (18) is of the same form as Eq. (10), and by means of the solution (11), we get

$$\tau^*_{w1} = \frac{1}{k^*_2}\left[\frac{1}{B}W\left(Be^{V+B}\right) - 1\right], \tag{19}$$

where

$$B \equiv \frac{H^*}{\eta^*(k^*_1 + k'^*_1)k^*_2} \tag{20}$$

is the "logarithmic" slip number and

$$V \equiv \frac{V^*}{k^*_1 + k'^*_1}. \tag{21}$$

It should be noted that in the case of no slip, the logarithmic slip number tends to infinity. In the following, we scale velocities by k^*_1 and y^* by H^*. Taking into account Eq. (18), the dimensionless slip velocities are given by

$$u_{w1} = V + B - W\left(Be^{V+B}\right), \quad u_{w2} = \gamma u_{w1}, \tag{22}$$

where

$$\gamma \equiv \frac{k'^*_1}{k^*_1}. \tag{23}$$

[Since $u_{w1} < V$, it is deduced that $W(Be^{V+B}) > B$.] Substituting into Eq. (14) and rearranging, we get the dimensionless velocity profile,

$$u_x(y) = (1+\gamma)\left[W\left(Be^{V+B}\right) - B\right]y + V + B - W\left(Be^{V+B}\right). \tag{24}$$

In order to investigate the effect of logarithmic slip on the flow, we consider the case where the same slip law applies to both walls, $k'^*_1 = k^*_1$ and thus $\gamma = 1$. The dimensionless slip velocities in Eq. (22) are then equal, and the dimensionless velocity profile is given by

$$u_x(y) = 2\left[W\left(Be^{V+B}\right) - B\right]y + V + B - W\left(Be^{V+B}\right). \tag{25}$$

The dimensionless slip velocity, u_w, is plotted vs the dimensionless plate velocity, $V = V^*/(2k^*_1)$, in Fig. 3(a) for various values of the slip number B. As expected, slip is enhanced as the latter number is reduced (when V is fixed, reducing B is equivalent to increasing k^*_2). Scaling the slip velocity by V^* (instead of k^*_1) leads to Fig. 3(b), where it can be observed that the effect of slip becomes less important as the plate speed is increased. Note that as $B \to 0$, the velocity profile tends to become uniform and $u^*_x/V^* \to 1/2$. This is also illustrated in Fig. 4, where dimensionless velocity profiles (u^*_x scaled by V^*) are plotted for $B = 10$ (weak slip), $B = 1$ (moderate slip), and $B = 0.1$ (strong slip) and various values of V.

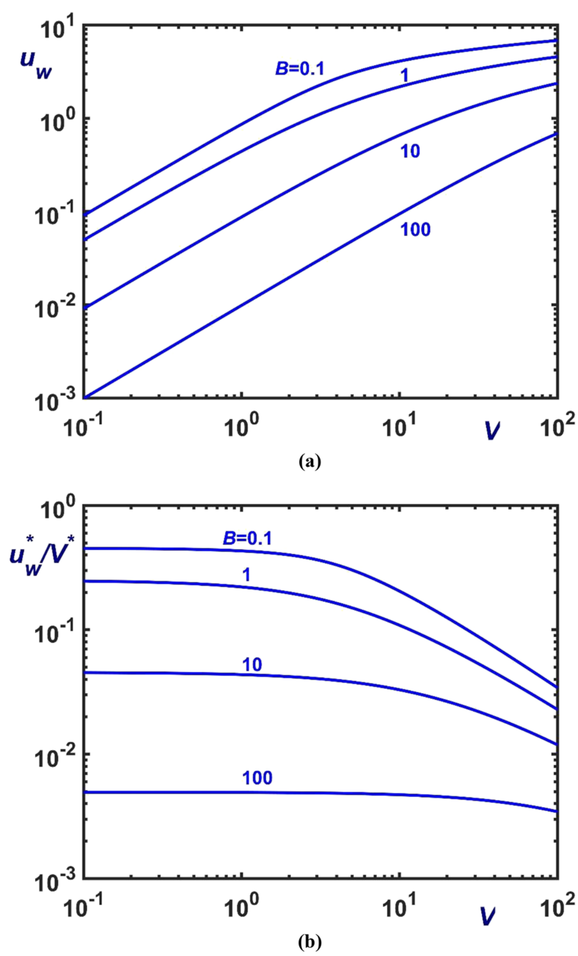

FIG. 3. (a) Dimensionless slip velocity as a function of the dimensionless speed of the moving plate (both scaled by k^*_1) in the simple shear flow for various values of the slip number B. (b) Same plot but now the slip velocity is scaled by the velocity V^* of the upper plate. The same logarithmic law is applied along the two walls.

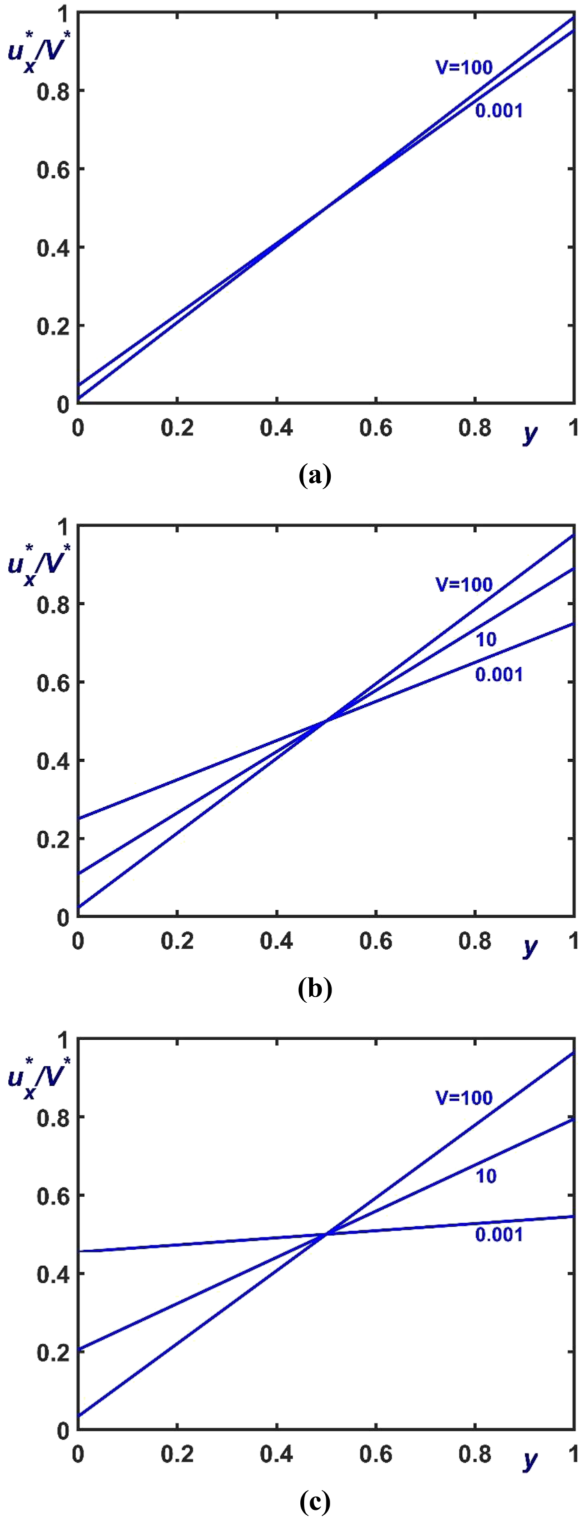

FIG. 4. Dimensionless velocity profiles for various values of the dimensionless speed of the upper plate in the simple shear flow: (a) B = 10, (b) B = 1, and (c) B = 0.1. The same logarithmic law is applied along the two walls.

IV. POISEUILLE FLOWS

A. Plane Poiseuille flow

Consider the plane Poiseuille flow in the presence of wall slip under the assumption that the same slip law applies at both walls so that the flow remains symmetric. It is easily shown that the velocity and the shear stress are given by[32]

$$u_x^* = u_w^* + \frac{G^*}{2\eta^*}\left(H^{*2} - y^{*2}\right), \quad \tau_{yx}^* = -G^* y^*, \tag{26}$$

where $G^* = (-dp^*/dx^*)$ is the pressure gradient and H^* is the channel half-width. The wall shear stress is $\tau_w^* = \left|\tau_{yx}^*\right|_{y^*=H^*} = G^* H^*$, and the volumetric flow rate $Q^* \equiv 2w^* \int_0^{H^*} u_x^* dy^*$, where w^* is the width of the channel in the transverse direction, is

$$Q^* = 2w^* H^* \left(u_w^* + \frac{H^{*2} G^*}{3\eta^*}\right). \tag{27}$$

The above expressions hold for any slip equation and for the no-slip case, where $u_w^* = 0$. In the case of logarithmic slip,

$$u_w^* = k_1^* \ln\left(1 + k_2^* H^* G^*\right). \tag{28}$$

Substituting Eq. (28) into Eq. (27) gives

$$\frac{Q^*}{2w^* H^*} = k_1^* \ln\left(1 + k_2^* H^* G^*\right) + \frac{H^{*2} G^*}{3\eta^*}. \tag{29}$$

This equation is of the form (10), and therefore, one can solve for the pressure gradient in terms of the desired volumetric flow rate,

$$G^* = \frac{3\eta^* k_1^*}{H^{*2}} W\left(\frac{H^*}{3\eta^* k_1^* k_2^*} e^{\frac{Q^*}{2w^* k_1^* H^*} + \frac{H^*}{3\eta^* k_1^* k_2^*}}\right) - \frac{1}{k_2^* H^*}. \tag{30}$$

The dimensionless form of the above equation when the pressure gradient is scaled by $3\eta^* k_1^*/H^{*2}$ is

$$G = W\left(B e^{V+B}\right) - B, \tag{31}$$

where $V \equiv Q^*/(2w^* k_1^* H^*)$ is the dimensionless mean velocity in the channel and $B \equiv H^*/(3\eta^* k_1^* k_2^*)$ is the slip number.

B. Axisymmetric Poiseuille flow

Similarly, in axisymmetric Poiseuille flow with wall slip, the velocity and the shear stress are given by

$$u_z^* = u_w^* + \frac{G^*}{4\eta^*}\left(R^{*2} - r^{*2}\right), \quad \tau_{zr}^* = -\frac{1}{2} G^* r^*, \tag{32}$$

where $G^* = (-dp^*/dz^*)$ is the pressure gradient and R^* is the radius of the tube. The wall shear stress is $\tau_w^* = G^* R^*/2$, while the volumetric flow rate is given by

$$Q^* = \pi R^{*2}\left(u_w^* + \frac{R^{*2} G^*}{8\eta^*}\right), \tag{33}$$

and thus, under the assumption of logarithmic slip,

$$\frac{Q^*}{\pi R^{*2}} = k_1^* \ln\left(1 + k_2^* H^* G^*/2\right) + \frac{R^{*2} G^*}{8\eta^*}. \tag{34}$$

Solving for G^* gives

$$G^* = \frac{8\eta^* k_1^*}{R^{*2}} W\left(\frac{R^*}{4\eta^* k_1^* k_2^*} e^{\frac{Q^*}{\pi R^{*2} k_1^*} + \frac{R^*}{4\eta^* k_1^* k_2^*}}\right) - \frac{2}{k_2^* R^*}. \tag{35}$$

When scaling the pressure gradient by $8\eta^* k_1^*/R^{*2}$, we find that the dimensionless pressure gradient is given by Eq. (31), where now $V \equiv Q^*/(\pi R^{*2} k_1^*)$ and $B \equiv R^*/(4\eta^* k_1^* k_2^*)$.

V. ANNULAR COUETTE FLOW

In this section, we consider the annular Couette flow, i.e., the flow between two infinitely long coaxial cylinders of radii R^* and κR^*, where $0 < \kappa < 1$, which is driven by the axial motion of the inner cylinder, as illustrated in Fig. 5. It is easily shown that for a Newtonian fluid, the velocity and the shear stress are given by[32]

$$u_z^* = c_1^* \ln r^* + c_2^*, \quad \tau_{zr}^* = -\frac{\eta c_1^*}{r^*}, \tag{36}$$

where c_1^* and c_2^* are integration constants to be determined by applying the boundary conditions. It is easily deduced that $\tau_{w2}^* = \kappa\tau_{w1}^*$, i.e., $\tau_{w2}^* < \tau_{w1}^*$. Hence, when the same slip law applies at both cylinders, the material is expected to slip more at the inner than the outer cylinder.

In the general case of wall slip along both cylinders, the boundary conditions read:

$$u_z^*(\kappa R^*) = V^* - u_{w1}^* \text{ and } u_z^*(R^*) = u_{w2}^*, \tag{37}$$

where u_{w1}^* and u_{w2}^* are the slip velocities at the inner and outer cylinders, respectively. Applying the boundary conditions and eliminating the integration constants yield

$$u_z^* = \frac{V^* - u_{w1}^* - u_{w2}^*}{\ln(1/\kappa)} \ln\frac{R^*}{r^*} + u_{w2}^* \tag{38}$$

and

$$\tau_{zr}^* = \eta^* \frac{du_z^*}{dr^*} = -\frac{\eta^*\left(V^* - u_{w1}^* - u_{w2}^*\right)}{\ln(1/\kappa) r^*}. \tag{39}$$

Therefore, for the shear stresses at the inner and outer cylinders, we get

$$\tau_{w1}^* = \frac{\eta^*\left(V^* - u_{w1}^* - u_{w2}^*\right)}{\ln(1/\kappa)\kappa R^*}, \quad \tau_{w2}^* = \kappa\tau_{w1}^*. \tag{40}$$

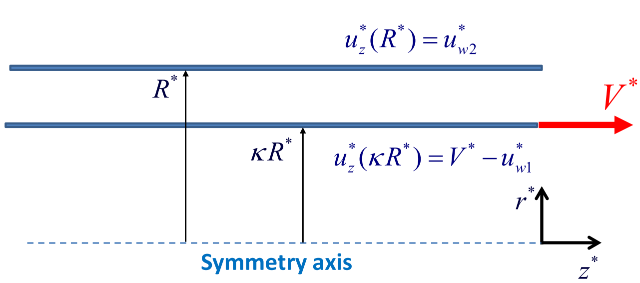

FIG. 5. Geometry and boundary conditions of the annular Couette flow with slip along both walls.

In general, applying the slip equations governing slip at the two cylinders and making use of Eq. (40) lead to an algebraic system for the two slip velocities u_{w1}^* and u_{w2}^*, which can be solved using standard numerical methods. In the case of logarithmic laws holding at the two walls, i.e., when

$$u_{w1}^* = k_1^* \ln\left(1 + k_2^* \tau_{w1}^*\right), \quad u_{w2}^* = k_1'^* \ln\left(1 + k_2'^* \tau_{w2}^*\right), \tag{41}$$

where $k_1'^*$ and $k_2'^*$ are the slip coefficients at the outer cylinder, substituting from Eq. (40) yields the following nonlinear system:

$$u_{w1}^* = k_1^* \ln\left[1 + \frac{k_2^* \eta^*\left(V^* - u_{w1}^* - u_{w2}^*\right)}{\ln(1/\kappa)\kappa R^*}\right] \tag{42}$$

and

$$u_{w2}^* = k_1'^* \ln\left[1 + \frac{k_2'^* \eta^*\left(V^* - u_{w1}^* - u_{w2}^*\right)}{\ln(1/\kappa) R^*}\right]. \tag{43}$$

With the exception of the very special case where $k_2^* = \kappa k_2'^*$, the above system can only be solved numerically.

Nevertheless, analytical solutions can be obtained assuming that logarithmic slip occurs along one cylinder and no- or even Navier slip occurs along the other. In what follows, we assume that Navier slip takes along the outer wall such that

$$u_{w2}^* = \frac{\tau_{w2}^*}{\beta_2^*}. \tag{44}$$

Combining Eqs. (40) and (44), we find that

$$u_{w2}^* = \frac{B_2\left(V^* - u_{w1}^*\right)}{1 + B_2}, \tag{45}$$

where B_2 is the "outer" Navier slip number defined by

$$B_2 \equiv \frac{\eta^*}{\ln(1/\kappa)\beta_2^* R^*}. \tag{46}$$

It should be pointed out that B_2 vanishes in the case of no-slip, unlike the logarithmic-slip number in Eq. (20), which goes to infinity. Noting that

$$V^* - u_{w1}^* - u_{w2}^* = \frac{V^* - u_{w1}^*}{1 + B_2}, \tag{47}$$

expressions (38)–(40) for the velocity and the stresses become

$$u_z^* = \frac{V^* - u_{w1}^*}{1 + B_2}\left[\frac{\ln(R^*/r^*)}{\ln(1/\kappa)} + B_2\right], \tag{48}$$

$$\tau_{zr}^* = \frac{\eta^*\left(V^* - u_{w1}^*\right)}{\ln(1/\kappa)(1 + B_2) r^*}, \tag{49}$$

and

$$\tau_{w1}^* = \frac{\eta^*\left(V^* - u_{w1}^*\right)}{\ln(1/\kappa)(1 + B_2)\kappa R^*}. \tag{50}$$

Before deriving the solution when logarithmic slip occurs along the inner cylinder, it is instructive to solve the problem with Navier slip.

A. Navier slip along the inner cylinder

In this case, the inner slip velocity is given by

$$u_{w1}^* = \frac{\tau_{w1}^*}{\beta_1^*}. \tag{51}$$

Substituting into Eq. (50), one can first solve for u_{w1}^* and then find the following solution:

$$u_z^* = \frac{V^*}{1+B_1+B_2}\left[\frac{\ln(R^*/r^*)}{\ln(1/\kappa)} + B_2\right],$$
$$\tau_{zr}^* = -\frac{\eta^* V^*}{\ln(1/\kappa)(1+B_1+B_2)r^*}, \tag{52}$$

where

$$B_1 \equiv \frac{\eta^*}{\ln(1/\kappa)\beta_1^*\kappa R^*} \tag{53}$$

is the "inner" Navier slip number. The two slip velocities are as follows:

$$u_{w1}^* = \frac{B_1 V^*}{1+B_1+B_2}, \quad u_{w2}^* = \frac{B_2 V^*}{1+B_1+B_2}. \tag{54}$$

If the two slip coefficients are equal, i.e., if $\beta_1^* = \beta_2^*$, then $B_2 = \kappa B_1$, and the solution is simplified as follows:

$$u_z^* = \frac{V^*}{1+(1+\kappa)B_1}\left[\frac{\ln(R^*/r^*)}{\ln(1/\kappa)} + \kappa B_1\right]. \tag{55}$$

In addition, if there is no slip ($\beta_1^* = \beta_2^* \to \infty$ and thus $B_1 = B_2 = 0$), one gets the no-slip solution.

B. Logarithmic slip along the inner cylinder

In the case of logarithmic slip along the inner cylinder, the inner slip velocity is given by

$$u_{w1}^* = k_1^* \ln\left(1 + k_2^* \tau_{w1}^*\right). \tag{56}$$

Substituting τ_{w1}^* from Eq. (50), we get

$$u_{w1}^* = k_1^* \ln\left[1 + \frac{\eta^* k_2^* V^*}{\ln(1/\kappa)(1+B_2)\kappa R^*} - \frac{\eta^* k_2^*}{\ln(1/\kappa)(1+B_2)\kappa R^*} u_{w1}^*\right]. \tag{57}$$

Solving for u_{w1}^* gives

$$u_{w1}^* = V^* + k_1^* B_1(1+B_2) - k_1^* W\left[B_1(1+B_2)e^{V+B_1(1+B_2)}\right], \tag{58}$$

where

$$B_1 \equiv \frac{\ln(1/\kappa)\kappa R^*}{\eta^* k_1^* k_2^*} \tag{59}$$

is the inner logarithmic slip number and

$$V \equiv \frac{V^*}{k_1^*} \tag{60}$$

is the dimensionless velocity of the inner cylinder. Scaling the velocities with k_1^* leads to the dimensionless form of Eq. (58),

$$u_{w1} = V + B_1(1+B_2) - W\left[B_1(1+B_2)e^{V+B_1(1+B_2)}\right]. \tag{61}$$

From Eqs. (45) and (61), one finds that the outer slip velocity is given by

$$u_{w2} = B_2\left\{\frac{1}{1+B_2} W\left[B_1(1+B_2)e^{V+B_1(1+B_2)}\right] - B_1\right\}. \tag{62}$$

Substituting u_{w1} into Eq. (48), we get

$$u_z = \left\{\frac{1}{1+B_2} W\left[B_1(1+B_2)e^{V+B_1(1+B_2)}\right] - B_1\right\}\left[\frac{\ln(1/r)}{\ln(1/\kappa)} + B_2\right], \tag{63}$$

where we scaled the velocity by k_1^* and r^* by R^*.

If there is no slip along the outer wall (i.e., $B_2 = 0$), the solution is simplified to

$$u_z = \left[W\left(B_1 e^{V+B_1}\right) - B_1\right]\frac{\ln(1/r)}{\ln(1/\kappa)}. \tag{64}$$

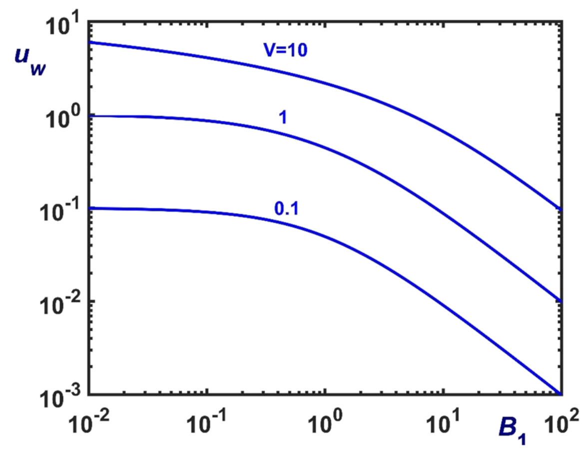

(a)

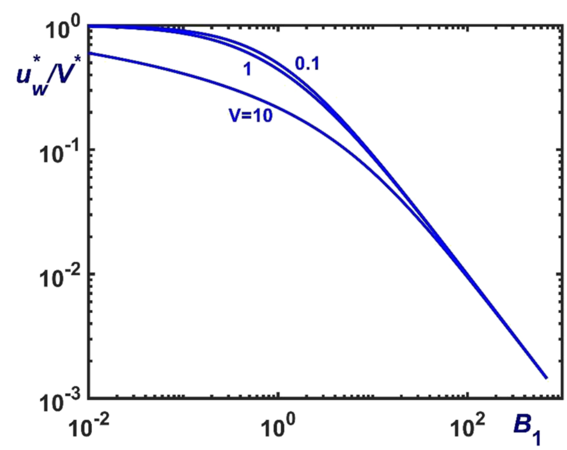

(b)

FIG. 6. Annular Couette flow (κ = 0.8) with logarithmic slip only along the inner cylinder (moving) and no-slip at the outer cylinder: (a) dimensionless slip velocity for various values of the dimensionless velocity V (both scaled by k_1^*) as a function of the slip number B_1 and (b) same plot but now the slip velocity is scaled by the velocity V^* of the inner cylinder.

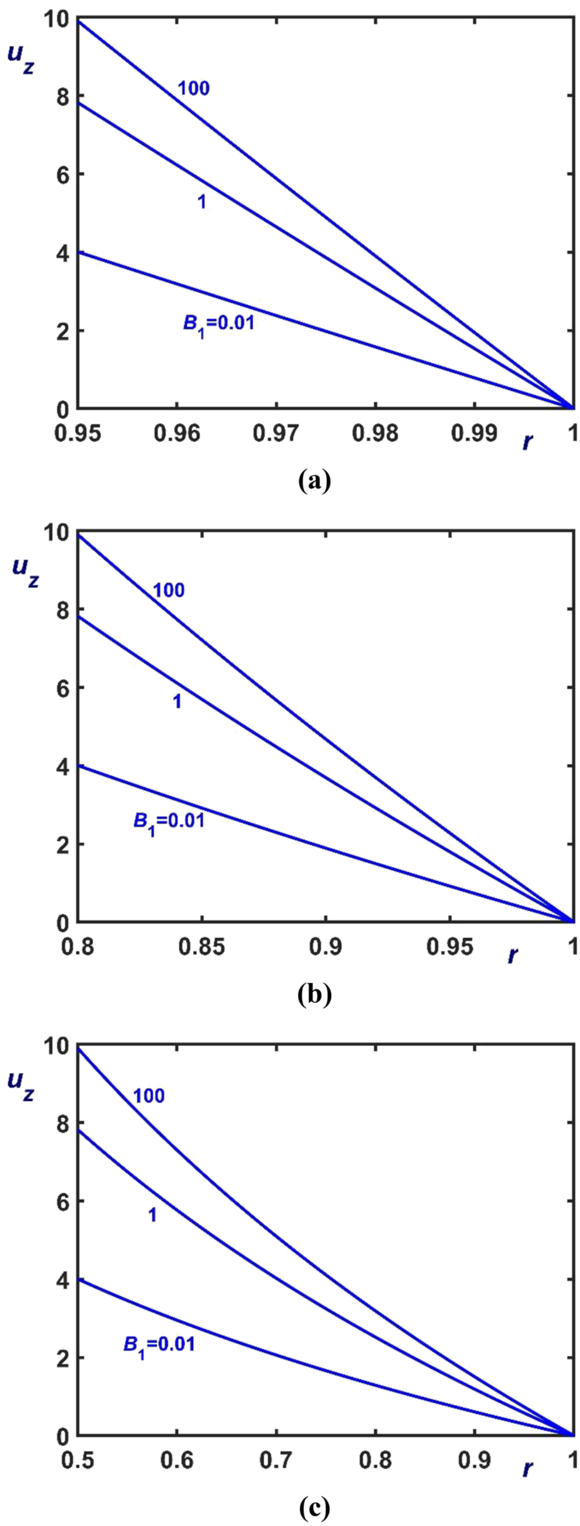

FIG. 7. Velocity profiles in the annular Couette flow with logarithmic slip only along the inner (moving) cylinder for $V = 10$ and various values of the slip number B_1: (a) $\kappa = 0.95$, (b) $\kappa = 0.8$, and (c) $\kappa = 0.5$.

By making use of the identity,

$$W(x) = \ln \frac{x}{W(x)}, \quad x > 0, \tag{65}$$

(which is valid for the positive part of the principal branch of the Lambert function), Eq. (64) may be written as follows:

$$u_z = \left[V + \ln \frac{B_1}{W(B_1 e^{V+B_1})} \right] \frac{\ln(1/r)}{\ln(1/\kappa)}. \tag{66}$$

The no-slip solution may be obtained taking the limit as $B_1 \to \infty$,

$$u_z = \frac{V \ln(1/r)}{\ln(1/\kappa)}. \tag{67}$$

Some results obtained assuming that there is no slip at the outer wall, i.e., using Eq. (64), are illustrated in Figs. 6 and 7. It should be noted that in this case, the slip velocity is given by Eq. (22), i.e.,

$$u_w = V + B_1 - W\left(B_1 e^{V+B_1}\right). \tag{68}$$

Therefore, Fig. 3(a) also applies for this flow. In Fig. 3(b), however, u_x^*/V^* should be multiplied by a factor of 2 due to the different scalings used [compare Eqs. (21) and (60)]. It should be pointed out that the effect of the radius ratio, κ, on the slip velocity is hidden in the slip number B_1, which is defined in Eq. (59). In Fig. 6(a), the dimensionless slip velocity u_w is plotted vs the slip number for $V = 0.1$, 1, and 10. When plotting u_x^*/V^* vs B_1 [Fig. 6(b)], we observe that the three curves coincide for high values of B_1 (weak to no slip), and they all tend to 1 as $B_1 \to 0$ (full slip limit). In Fig. 7, representative profiles are given for three radii ratios, $\kappa = 0.95$, 0.8 and 0.5, $V = 10$ and three values of the slip number, i.e., $B_1 = 100$, 1, and 0.01, corresponding to very weak, moderate, and strong slip, respectively, along the moving inner cylinder.

The solution for the annular Couette flow when logarithmic and Navier slip laws are applied along the outer and the cylinder, respectively, is presented in Appendix A.

VI. CIRCULAR COUETTE FLOW

Let us now consider the circular Couette flow with slip along the two coaxial, infinitely long cylinders containing a Newtonian fluid. It is assumed that the inner cylinder of radius κR^* rotates steadily at an angular velocity Ω^*, while the outer cylinder of radius R^* is fixed. The geometry of the flow is illustrated in Fig. 8. The azimuthal velocity and the shear stress are of the following general forms:[32]

$$u_\theta^* = c_1^* r^* + \frac{c_2^*}{r^*}, \quad \tau_{r\theta}^* = -\frac{2\eta^* c_2^*}{r^{*2}}, \tag{69}$$

where c_1^* and c_2^* are integration constants. It can be observed that $\tau_{w2}^* = \kappa^2 \tau_{w1}^*$.

In the presence of wall slip, the boundary conditions are

$$u_\theta^*(\kappa R^*) = \Omega^* \kappa R^* - u_{w1}^* \text{ and } u_\theta^*(R^*) = u_{w2}^* \tag{70}$$

where u_{w1}^* and u_{w2}^* are the slip velocities at the inner and outer cylinders, respectively. Applying the two boundary conditions leads to a system for c_1^* and c_2^*, the solution of which is

$$c_1^* = \frac{\kappa u_{w1}^* + u_{w2}^* - \Omega^* \kappa^2 R^*}{(1-\kappa^2) R^*}, \quad c_2^* = \frac{\kappa R^* \left(\Omega^* \kappa R^* - u_{w1}^* - \kappa u_{w2}^*\right)}{1-\kappa^2}. \tag{71}$$

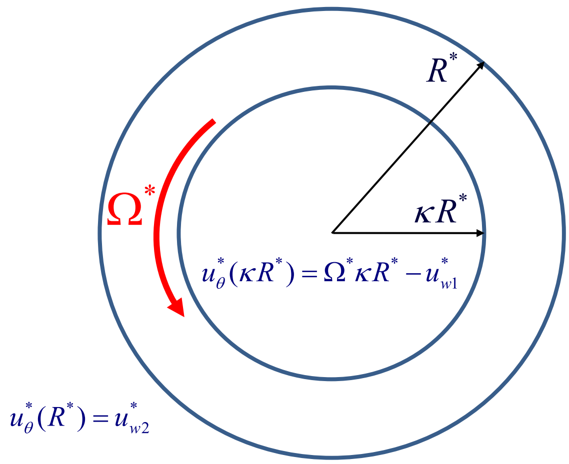

FIG. 8. Geometry and boundary conditions of the circular Couette flow with slip along both walls.

Substituting Eq. (71) into Eq. (69) gives

$$u_\theta^* = \frac{r^*}{(1-\kappa^2)R^*}\left[\kappa u_{w1}^* + u_{w2}^* - \Omega^*\kappa^2 R^* + \kappa\left(\Omega^*\kappa R^* - u_{w1}^* - \kappa u_{w2}^*\right)\frac{R^{*2}}{r^{*2}}\right] \quad (72)$$

and

$$\tau_{r\theta}^* = -\frac{2\eta^*\kappa R^*\left(\Omega^*\kappa R^* - u_{w1}^* - \kappa u_{w2}^*\right)}{(1-\kappa^2)r^{*2}}. \quad (73)$$

Hence, for the two wall shear stresses, we get

$$\tau_{w1}^* = \frac{2\eta^*\left(\Omega^*\kappa R^* - u_{w1}^* - \kappa u_{w2}^*\right)}{(1-\kappa^2)\kappa R^*}, \quad \tau_{w2}^* = \kappa^2\tau_{w1}^*. \quad (74)$$

As with the annular Couette flow, there is no analytical solution when logarithmic slip applies at the two cylinders. Below, we consider the case where Navier slip occurs along the outer cylinder, i.e., Eq. (44) applies. Substituting τ_{w2}^* from Eq. (74) and solving for u_{w2}^* give

$$u_{w2}^* = \frac{B_2\left(\Omega^*\kappa R^* - u_{w1}^*\right)}{1+\kappa B_2}, \quad (75)$$

where

$$B_2 \equiv \frac{2\eta^*\kappa}{(1-\kappa^2)R^*\beta_2^*}. \quad (76)$$

Substituting u_{w2}^* into Eqs. (72)–(74), we have

$$u_\theta^* = \frac{\left(\Omega^*\kappa R^* - u_{w1}^*\right)r^*}{(1-\kappa^2)(1+\kappa B_2)R^*}\left[B_2(1-\kappa^2) + \kappa\left(\frac{R^{*2}}{r^{*2}} - 1\right)\right], \quad (77)$$

$$\tau_{r\theta}^* = -\frac{2\eta^*\kappa R^*\left(\Omega^*\kappa R^* - u_{w1}^*\right)}{(1-\kappa^2)(1+\kappa B_2)r^{*2}}. \quad (78)$$

Hence, for the wall shear stresses, we get

$$\tau_{w1}^* = \frac{2\eta^*\left(\Omega^*\kappa R^* - u_{w1}^*\right)}{(1-\kappa^2)(1+\kappa B_2)\kappa R^*}, \quad \tau_{w2}^* = \kappa^2\tau_{w1}^*. \quad (79)$$

Below, we derive the solutions corresponding to the Navier and logarithmic slip law along the inner cylinder.

A. Navier slip along the inner cylinder

Applying Navier slip at the inner cylinder (51), we find the following expression for the inner slip velocity:

$$u_{w1}^* = \frac{B_1\Omega^*\kappa R^*}{1+B_1+\kappa B_2}, \quad (80)$$

where

$$B_1 \equiv \frac{2\eta^*}{(1-\kappa^2)\beta_1^*\kappa R^*}. \quad (81)$$

Substituting Eq. (80) into Eq. (77) gives

$$u_\theta^* = \frac{\Omega^*\kappa r^*}{(1-\kappa^2)(1+B_1+\kappa B_2)}\left[B_2(1-\kappa^2) + \kappa\left(\frac{R^{*2}}{r^{*2}} - 1\right)\right], \quad (82)$$

while the shear stress is given by

$$\tau_{r\theta}^* = -\frac{2\eta^*\Omega^*\kappa^2 R^{*2}}{(1-\kappa^2)(1+B_1+\kappa B_2)r^{*2}}. \quad (83)$$

In the case of no slip, $B_1 = B_2 = 0$, Eq. (82) is simplified as follows:

$$u_\theta^* = \frac{\Omega^*\kappa^2 r^*}{1-\kappa^2}\left(\frac{R^{*2}}{r^{*2}} - 1\right). \quad (84)$$

B. Logarithmic slip along the inner cylinder

Combining the logarithmic slip law (56) and Eq. (79), we get

$$u_{w1}^* = k_1^*\ln\left[1 + \frac{2\eta^* k_2^*\Omega^*}{(1-\kappa^2)(1+\kappa B_2)} - \frac{2\eta^* k_2^*}{(1-\kappa^2)(1+\kappa B_2)\kappa R^*}u_{w1}^*\right], \quad (85)$$

the solution of which is

$$u_{w1}^* = \Omega^*\kappa R^* + k_1^* B_1(1+\kappa B_2) - k_1^* W\left[B_1(1+\kappa B_2)e^{\Omega^*\kappa R^*/k_1^* + B_1(1+\kappa B_2)}\right], \quad (86)$$

where now

$$B_1 \equiv \frac{(1-\kappa^2)\kappa R^*}{2\eta^* k_1^* k_2^*}. \quad (87)$$

Scaling the velocities by k_1^*, the dimensionless form of Eq. (86) is

$$u_{w1} = V + B_1(1+\kappa B_2) - W\left[B_1(1+\kappa B_2)e^{V + B_1(1+\kappa B_2)}\right], \quad (88)$$

where

$$V \equiv \frac{\Omega^*\kappa R^*}{k_1^*}. \quad (89)$$

It is easily deduced from Eqs. (75) and (88) that Eq. (62) for the outer slip velocity u_{w2} in the annular Couette flow also holds for

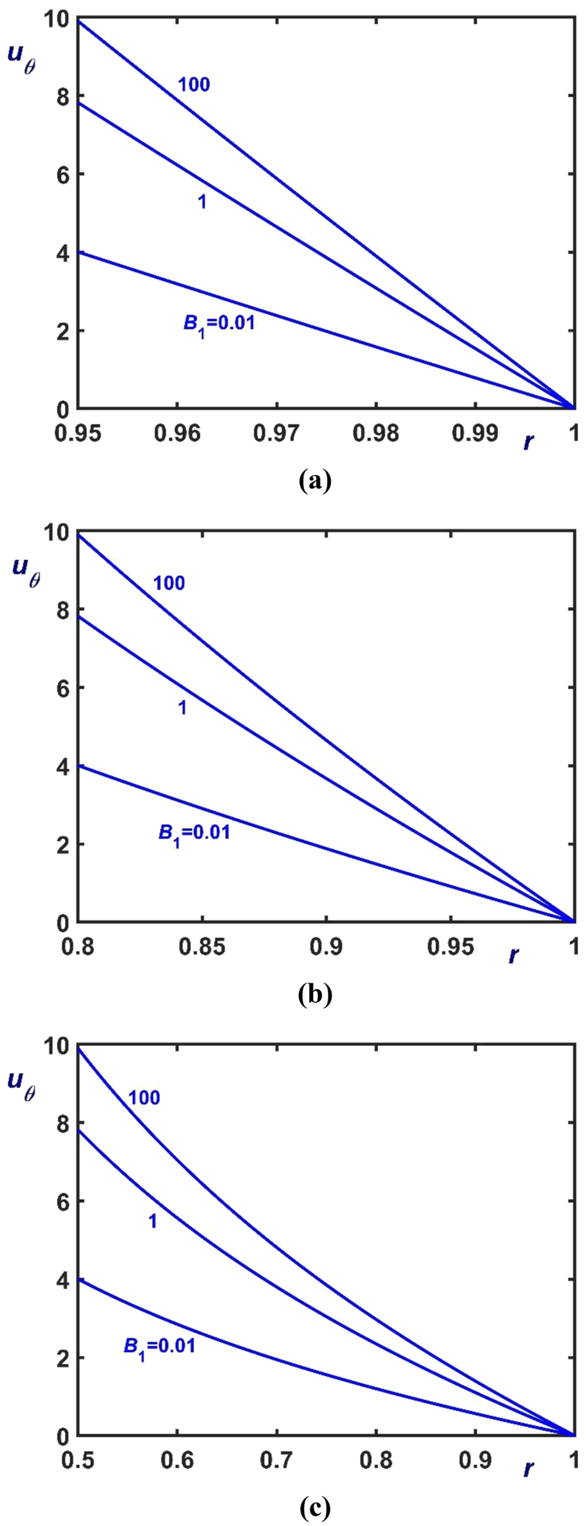

FIG. 9. Velocity profiles in the circular Couette flow with logarithmic slip only along the inner (rotating) cylinder for $V = 10$ and various values of the slip number B_1: (a) $\kappa = 0.95$, (b) $\kappa = 0.8$, and (c) $\kappa = 0.5$.

this flow problem. However, the definitions of the slip numbers are different.

Substituting into Eq. (77) and scaling r^* by R^*, we get

$$u_\theta = \frac{r}{1-\kappa^2}\left\{\frac{1}{1+\kappa B_2} W\left[B_1(1+\kappa B_2)e^{V+B_1(1+\kappa B_2)}\right] - B_1\right\} \times \left[B_2(1-\kappa^2) + \kappa\left(\frac{1}{r^2} - 1\right)\right]. \tag{90}$$

The dimensionless shear stress (scaled by k_2^{*-1}) is given by

$$\tau_{r\theta} = -\frac{1}{B_1}\left\{\frac{1}{1+\kappa B_2} W\left[B_1(1+\kappa B_2)e^{V+B_1(1+\kappa B_2)}\right] - B_1\right\}\frac{\kappa^2}{r^2}. \tag{91}$$

In the case of no slip along the outer cylinder ($B_2 = 0$), Eq. (90) becomes

$$u_\theta = \frac{\kappa r}{1-\kappa^2}\left[W\left(B_1 e^{V+B_1}\right) - B_1\right]\left(\frac{1}{r^2} - 1\right). \tag{92}$$

It is interesting to note that the effect of slip is actually the same as in the case of the annular Couette flow. Indeed, in both Eqs. (64) and (92), the no-slip solution is simply multiplied by the same factor $[W(B_1 e^{V+B_1}) - B_1]$. Moreover, the slip velocity in both cases is given by Eq. (68), where $V = V^*/k_1^*$ in annular flow and $V = \Omega^* \kappa R^*/k_1^*$ in circular Couette flow, respectively. Note, however, the slightly different definitions of B_1. Therefore, Figs. 3(a) and 6 also hold for the circular Couette flow. In Fig. 9, velocity profiles for $V = 10$ and $\kappa = 0.95$, 0.8, and 0.5 are provided for various slip numbers.

The solution for the circular Couette flow when logarithmic and Navier slip laws are applied along the outer and the cylinder, respectively, is presented in Appendix B.

VII. CONCLUSIONS

We have employed the Lambert W function to derive analytical solutions of the plane, annular, and circular Couette and plane and axisymmetric Poiseuille flows of a Newtonian fluid in the presence of wall slip described by a logarithmic slip law. In Poiseuille flows, analytical expressions of the pressure drop in terms of the volumetric flow rate have been provided. In annular and circular Couette flows, solutions are derived only for the case where logarithmic slip occurs along one cylinder, while Navier or no slip applies along the other one. Solutions corresponding to Navier slip have also been derived for comparison purposes. These solutions may be useful in rheometry, that is, for the rheological characterization of materials exhibiting logarithmic wall slip. The effects of the dimensionless slip numbers on the velocity distributions have been investigated and discussed.

APPENDIX A: ANNULAR COUETTE FLOW WITH LOGARITHMIC SLIP ALONG THE OUTER CYLINDER

Consider the annular Couette flow of Sec. V with the Navier and logarithmic slip along the inner and outer cylinders, respectively,

$$u_{w1}^* = \frac{\tau_{w1}^*}{\beta_1^*}, \quad u_{w2}^* = k_1^* \ln\left(1 + k_2^* \tau_{w2}^*\right). \tag{A1}$$

Working as in Sec. V, we obtain the following solution for the dimensionless velocity (scaled by k_1^*):

$$u_z = V - \left\{\frac{1}{1+B_1} W\left[B_2(1+B_1)e^{V+B_2(1+B_1)}\right] - B_2\right\} \times \left[1 + B_1 - \frac{\ln(1/r)}{\ln(1/\kappa)}\right], \quad \text{(A2)}$$

where the inner (Navier) and outer (logarithmic) slip numbers are defined by

$$B_1 \equiv \frac{\eta^*}{\kappa \ln(1/\kappa)\beta_1^* R^*}, \quad B_2 \equiv \frac{\ln(1/\kappa)R^*}{\eta^* k_1^* k_2^*}. \quad \text{(A3)}$$

The two slip velocities are given by

$$u_{w1} = B_1\left\{W\left[B_2(1+B_1)e^{V+B_2(1+B_1)}\right] - B_2\right\} \quad \text{(A4)}$$

and

$$u_{w2} = V + B_2(1+B_1) - W\left[B_2(1+B_1)e^{V+B_2(1+B_1)}\right]. \quad \text{(A5)}$$

Finally, the dimensionless shear stress (scaled by k_2^{*-1}) is

$$\tau_{zr} = \left\{1 - \frac{1}{B_2(1+B_1)} W\left[B_2(1+B_1)e^{V+B_2(1+B_1)}\right]\right\}\frac{1}{r}. \quad \text{(A6)}$$

Setting $B_1 = 0$ yields the solution when no slip occurs at the moving inner cylinder.

APPENDIX B: CIRCULAR COUETTE FLOW WITH LOGARITHMIC SLIP ALONG THE OUTER CYLINDER

Let us consider the circular Couette flow of Sec. VI when Navier slip occurs along the inner rotating cylinder and logarithmic slip along the outer fixed cylinder, following Eq. (A1). The dimensionless azimuthal velocity is found to be

$$u_\theta = r\left\{V - \frac{W\left[B_2(1+B_1)e^{V+B_2(1+B_1)}\right] - B_2}{1-\kappa^2}\left[1 + (1-\kappa^2)B_1 - \frac{\kappa^2}{r^2}\right]\right\}, \quad \text{(B1)}$$

where the slip numbers are defined by

$$B_1 \equiv \frac{2\eta^*}{\kappa(1-\kappa^2)\beta_1^* R^*}, \quad B_2 \equiv \frac{(1-\kappa^2)R^*}{2\kappa^2\eta^* k_1^* k_2^*} \quad \text{(B2)}$$

and

$$V \equiv \frac{\Omega^* R^*}{k_1^*}. \quad \text{(B3)}$$

The inner slip velocity is

$$u_{w1} = \kappa B_1\left\{\frac{1}{1+B_1} W\left[B_2(1+B_1)e^{V+B_2(1+B_1)}\right] - B_2\right\}, \quad \text{(B4)}$$

while the outer slip velocity is given by Eq. (A5) for the annular Couette flow keeping in mind the different definitions of B_1, B_2, and V. Finally, the dimensionless shear stress (scaled by k_2^{*-1}) is

$$\tau_{r\theta} = \left\{1 - \frac{1}{B_2(1+B_1)} W\left[B_2(1+B_1)e^{V+B_2(1+B_1)}\right] - 1\right\}\frac{1}{r^2}. \quad \text{(B5)}$$

The similarity of Eqs. (A6) and (B1) should be noted. Setting $B_1 = 0$ yields the solution when no slip occurs at the moving inner cylinder.

DATA AVAILABILITY

The data that support the findings of this study are available from the corresponding author upon reasonable request.

REFERENCES

[1] S. G. Hatzikiriakos, "Slip mechanisms in complex fluid flows," Soft Matter **11**, 7851–7856 (2015).
[2] S. G. Hatzikiriakos, "Wall slip of molten polymers," Prog. Polym. Sci. **37**, 624–643 (2012).
[3] M. Ebrahimi, V. K. Konaganti, and S. G. Hatzikiriakos, "Dynamic slip of polydisperse linear polymers using partitioned plate," Phys. Fluids **30**, 030601 (2018).
[4] A. Y. Malkin and S. A. Patlazhan, "Wall slip for complex liquids - phenomenon and its causes," Adv. Colloid Interface Sci. **257**, 42–57 (2018).
[5] C. Neto, D. R. Evans, E. Bonaccurso, H.-J. Butt, and V. S. J. Craig, "Boundary slip in Newtonian liquids: A review of experimental studies," Rep. Prog. Phys. **68**, 2859–2897 (2005).
[6] E. Bonaccurso, M. Kappl, and H. J. Butt, "Hydrodynamic force measurement: Boundary slip of water on hydrophilic surfaces and electrokinetic effects," Phys. Rev. Let. **88**, 076103 (2002).
[7] E. Lauga, M. P. Brenner, and H. A. Stone, "Microfluidics: The no-slip boundary condition," in *Handbook of Experimental Fluid Dynamics*, edited by C. Tropea, A. L. Yarin, and J. F. Foss (Springer, Heidelberg, 2007), pp. 1219–1240.
[8] M. M. Denn, "Extrusion instabilities and wall slip," Annu. Rev. Fluid Mech. **33**, 265–287 (2001).
[9] C. L. M. H. Navier, "Sur les lois du mouvement des fluids," Mem. Acad. R. Sci. Inst. France **6**, 389–440 (1827).
[10] W. R. Schowalter, "The behavior of complex fluids at solid boundaries," J. Non-Newtonian Fluid Mech. **29**, 25–36 (1988).
[11] H. Spikes and S. Granick, "Equation for slip of simple liquids at smooth solid surfaces," Langmuir **19**, 5065–5071 (2003).
[12] Y. Damianou, M. Philippou, G. Kaoullas, and G. C. Georgiou, "Cessation of viscoplastic Poiseuille flow with wall slip," J. Non-Newtonian Fluid Mech. **203**, 24–37 (2014).
[13] Y. Damianou, P. Panaseti, and G. C. Georgiou, "Viscoplastic Couette flow in the presence of wall slip with non-zero slip yield stress," Materials **12**, 3574 (2019).
[14] S. G. Hatzikiriakos, "A slip model for linear polymers based on adhesive failure," Int. Polym. Process. **8**, 135–142 (1993).
[15] ANSYS Polyflow manual (implementation of boundary conditions), ANSYS, 2011.
[16] L. L. Ferrás, J. M. Nóbrega, and F. T. Pinho, "Analytical solutions for Newtonian and inelastic non-Newtonian flows with wall slip," J. Non-Newtonian Fluid Mech. **175-176**, 76–88 (2012).
[17] G. Kaoullas and G. C. Georgiou, "Newtonian Poiseuille flows with slip and non-zero slip yield stress," J. Non-Newtonian Fluid Mech. **197**, 24–30 (2013).
[18] M. Philippou, Y. Damianou, X. Miscouridou, and G. C. Georgiou, "Cessation of Newtonian circular and plane Couette flows with wall slip and non-zero slip yield stress," Meccanica **52**, 2081–2099 (2017).
[19] R. M. Corless, G. H. Gonnet, D. A. Hare, D. J. Jeffrey, and D. E. Knuth, "On the Lambert W function," Adv. Comput. Math. **5**, 329–359 (1996).
[20] G. A. Davies and J. R. Stokes, "Thin film and high shear rheology of multiphase complex fluids," J. Non-Newtonian Fluid Mech. **148**, 73–87 (2008).
[21] A. Ahuja and A. Singh, "Slip velocity of concentrated suspensions in Couette flow," J. Rheol. **53**, 1461–1485 (2009).
[22] G. C. Georgiou, "On the stability of the shear flow of a viscoelastic fluid with slip along the fixed wall," Rheol. Acta **35**, 39–47 (1996).

[23]M. Piau and J. M. Piau, "Plane Couette flow of viscoplastic materials along a slippery vibrating wall," J. Non-Newtonian Fluid Mech. **125**, 71–85 (2005).
[24]G. Keady, "Colebrook-White formula for pipe flows," J. Hydraul. Eng. **124**, 96–97 (1998).
[25]A. A. More, "Analytical solutions for the Colebrook and White equation and for pressure drop in ideal gas flow in pipes," Chem. Eng. Sci. **61**, 5515–5519 (2006).
[26]A. Jaishankar and G. H. McKinley, "An analytical solution to the extended Navier–Stokes equations using the Lambert W function," AIChE J. **60**(4), 1413–1423 (2014).
[27]T. Massalha and R. M. Digilov, "Capillary viscometer with a pressure sensor: A subject for student projects," Eur. J. Phys. **36**, 065045 (2015).
[28]S. P. Pudasaini, "Some exact solutions for debris and avalanche flows," Phys. Fluids **23**, 043301 (2011).
[29]Z. You, R. R. Huilgol, and E. Mitsoulis, "Application of the Lambert W function to steady shearing flows of the Papanastasiou model," Int. J. Eng. Sci. **46**, 799–8002 (2008).
[30]A. Syrakos, Y. Dimakopoulos, G. C. Georgiou, and J. Tsamopoulos, "Viscoplastic flow in an extrusion damper," J. Non-Newtonian Fluid Mech. **232**, 102–124 (2016).
[31]J. Férec, E. Bertevas, B. C. Khoo, G. Ausias, and N. Phan-Thien, "A rheological constitutive model for semiconcentrated rod suspensions in Bingham fluids," Phys. Fluids **29**, 073103 (2017).
[32]T. Papanastasiou, G. Georgiou, and A. Alexandrou, *Viscous Fluid Flow* (CRC Press, Boca Raton, 2000).